Light-induced spiral mass transport in azo-polymer films under vortex-beam illumination – Supplementary Information

Antonio Ambrosio[a),1], Lorenzo Marrucci[1], Fabio Borbone[2], Antonio Roviello[2] and Pasqualino Maddalena[1]

1. CNR-SPIN and Dipartimento di Scienze Fisiche, Università degli Studi di Napoli Federico II, Via Cintia, 80126 Napoli, Italy

2. Dipartimento di Scienze Chimiche, Università degli Studi di Napoli Federico II, Via Cintia, 80126 Napoli, Italy

[a)]Electronic mail: antonio.ambrosio@spin.cnr.it

Supplementary figures

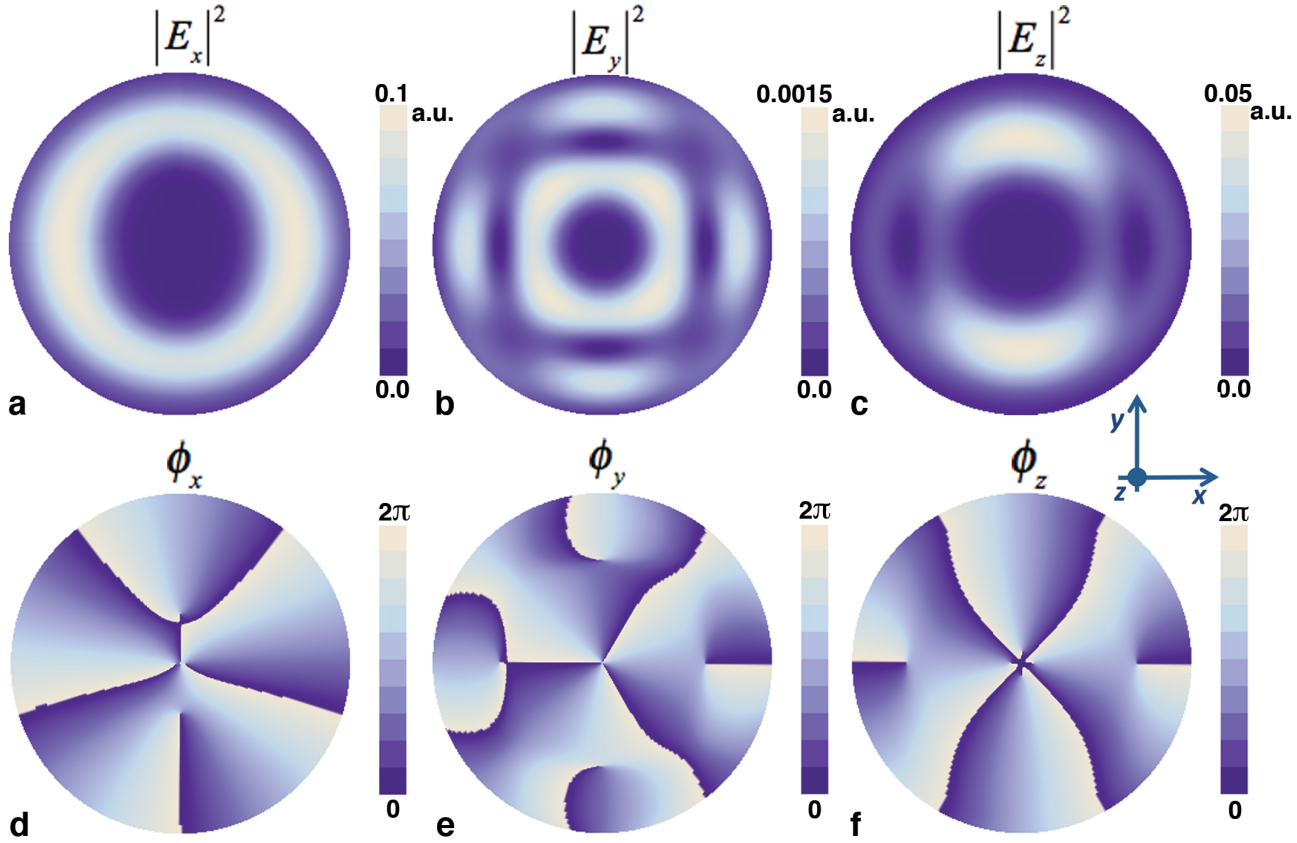

Supplementary Figure S1 | Field amplitude and phase at the focal plane. a, Simulated two-dimensional distribution of the $|E_x|^2$ component of a q = 5 Laguerre-Gauss beam at the focal plane of a oil-immersion 1.4 NA microscope objective (values in arbitrary units). The beam is linearly polarized along the x-azis. **b**, **c**, The same as **a** for the components $|E_y|^2$ and $|E_z|^2$ of the electromagnetic field. **d**, Optical phase around the beam propagation axis (z) for the E_x component of a q = 5 Laguerre-Gauss beam at the focal plane. **e**, **f**, The same as for **d** for the E_y and E_z components, respectively. The simulated area has a diameter of four optical wavelengths.

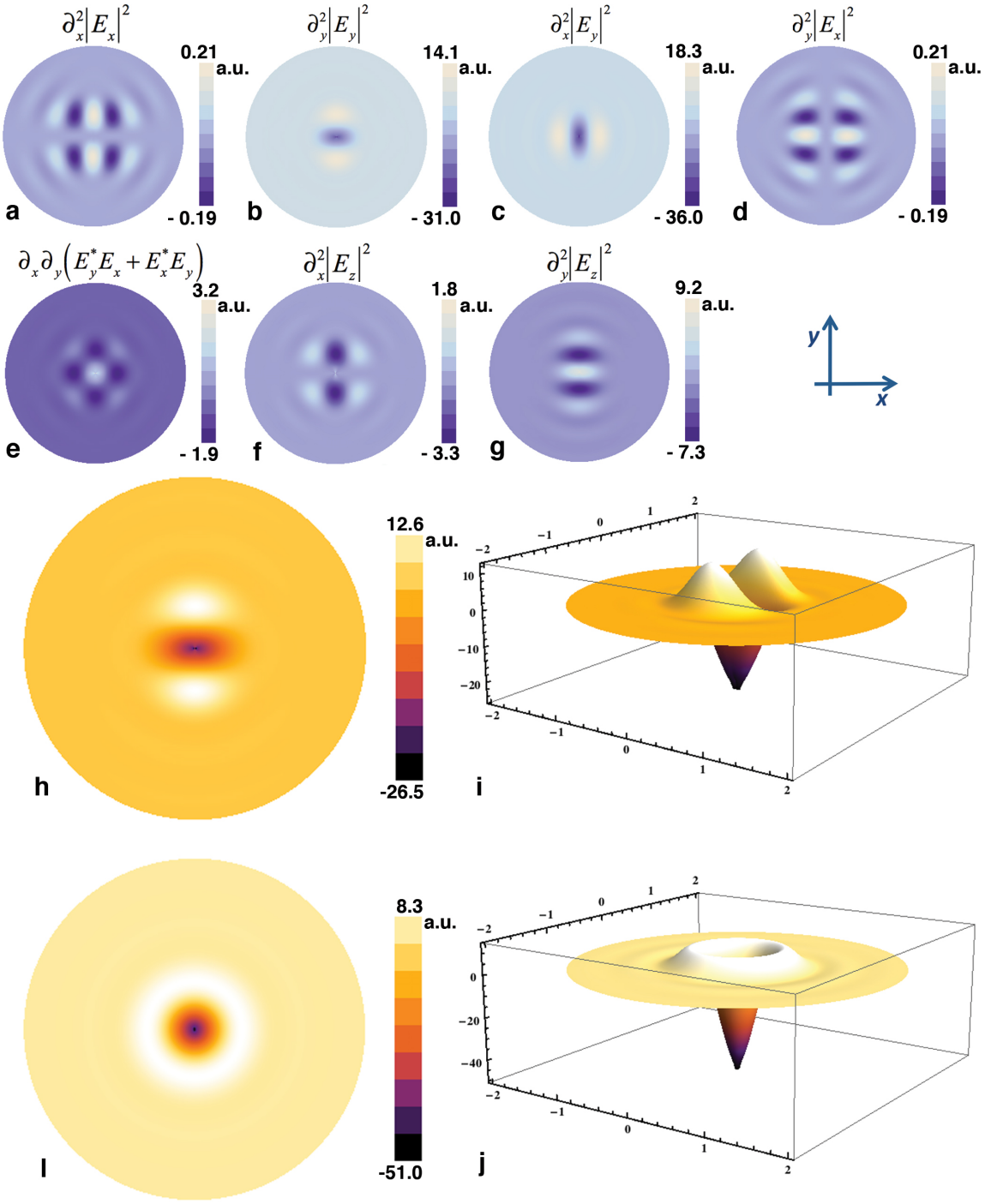

Supplementary Figure S2 | Material displacement due to a focused polarized Gaussiam beam. **a**, Simulation of the two-dimensional distribution at the focal plane for the quantity $\partial_x^2|E_x|^2$ in the case of a tightly-focused Gaussian laser beam, linearly polarized along the *y*-axis. **b**, **c**, **d**, **e**, **f**, **g**, The same as in **a** for the quantities reported above each distribution. **h**, Two-dimensional map of the height variation, $\Delta h(x,y)$, of the topographical structure obtained from our model (Eq. 2 of the main Article) by setting the constants' values to: $c_1 = 0$; $c_2 = 1$; $c_3 = 0$. **i**, Three-dimensional representation of the same distribution reported in **h**. The material displacement occurs mainly along the polarization direction. **l**, The same as for **h** in the case of illumination by means of a circularly polarized Gaussian beam. **j**, Three-dimensional representation of the same distribution reported in **l**. The simulated area has a diameter of four wavelengths.

Supplementary Methods

Phenomenological model of light-induced mass transport. Let us consider a polymer thin film deposited on a rigid substrate and initially extending in the region comprised between the plane z = 0 (polymer-substrate interface) and the plane $z = L$ (polymer free surface). Actually, it is possible that the polymer region in which the light-induced mass migration occurs does not correspond to the entire polymer thickness, in which case L will represent the effective thickness of this "mobile" region of the polymer and the plane $z = 0$ will correspond to an inner polymer layer at which no light-induced motion can take place. After exposure to light, the polymer develops surface reliefs, which can be described by the function $h(x,y)$ giving the new z-coordinate of the free surface, or equivalently by the height variations $\Delta h(x,y) = h(x,y) - L$. We assume that these surface reliefs arise as a consequence of light-induced mass transport, as described by a mass-current-density vector **J** determined by the optical field. We neglect possible additional contributions to the mass-current-density, such as visco-elastic interactions between adjacent moving regions of the polymer. This mass transport acts on the polymer by varying the local mass density ρ, which in turn determines a deformation of the polymer film via its elastic response. However, here we assume the validity of a simplified limit in which the light-induced mass density variations are exactly balanced by a local expansion (or contraction) of the polymer, so as to return to the initial equilibrium density, according to the following law (incompressibility approximation):

$$\frac{\Delta V}{V} = \partial_i u_i = \frac{\Delta \rho_{\text{light}}}{\rho} \quad \text{(S1)}$$

where u_i is the elastic displacement vector and sum over repeated indices is assumed. Moreover, we assume that the film thickness L is much smaller than the imposed lateral variations of $\Delta\rho_{\text{light}}$ along x and y and hence the derivatives of u_i with respect to x and y can be neglected in Eq. (S1) (this assumption will be valid if the effective thickness L is much smaller than the laser spot-size). These assumptions yield

$$\partial_z u_z = \frac{\Delta \rho_{\text{light}}}{\rho} \quad \Rightarrow \quad u_z(L) = h(L) - L = \Delta h = \int_0^L \frac{\Delta \rho_{\text{light}}}{\rho} dz \simeq \frac{1}{\rho}\int_0^L \Delta \rho_{\text{light}}\, dz = \frac{L}{\rho}\overline{\Delta\rho} \quad \text{(S2)}$$

where $\overline{\Delta\rho}$ is the light-induced density variation averaged along z over the entire effective thickness and we have used the fact that the substrate is rigid, so that $u_z(0) = 0$. The link between the light-induced mass density variations and the light-induced current density **J** is provided by the mass continuity equation:

$$\frac{\partial \rho_{\text{light}}}{\partial t} = -\partial_i J_i \quad \Rightarrow \quad \frac{\partial \overline{\rho}}{\partial t} = -\frac{1}{L}\int_0^L \partial_i J_i\, dz = -\partial_k \overline{J}_k - \frac{1}{L}\left[J_z(L) - J_z(0)\right] = -\partial_k \overline{J}_k \quad (k = x,y) \quad \text{(S3)}$$

where we have introduced the averaged lateral currents $\overline{J}_k$ with k spanning only the two transverse coordinates x and y, while the current J_z is assumed to vanish at the bounding surfaces because there can be no mass transport out of the polymer. Combining Eqs. (S2) and (S3) and assuming an exposure time τ during which the light-induced current density is taken to remain constant, we obtain the following final expression of the reliefs which will be used in the following:

$$\Delta h(x,y) = -\frac{L\tau}{\rho}\partial_k \overline{J}_k \quad (k = x,y) \qquad \text{(S4)}$$

We can see from this equation that, in order to determine the surface reliefs, within the present approximation we only need to know the lateral current density induced by light, averaged over the polymer thickness. Precisely, we need to write a constitutive equation that gives the current density **J** resulting from a given applied optical field, as described by the electric field **E** and magnetic field **B**. We can exclude a linear dependence of **J** on **E** or **B**, as for a quasi-monochromatic field this term would average to zero. Therefore, the lowest-order dependence must be quadratic in the field components. Moreover, we can reasonably assume that the material response (being related with light absorption) is sensitive to the electric field **E** only, and not to the magnetic field, as the contribution of the latter to absorption is typically very weak. In particular, in the polymer bulk we can write the following fully general 3D constitutive equation, which assumes only isotropy of the polymer (at equilibrium), a lowest-order quadratic response on the optical field, and a lowest-order linear dependence of the field gradients:

$$J_i = C_1 \partial_i\left(E_j^* E_j\right) + C_2 \partial_j\left(E_j^* E_i\right) + C_2^* \partial_j\left(E_i^* E_j\right) \quad i = x,y,z \qquad \text{(S5)}$$

where C_1 and C_2 are two constants characteristic of the material and Maxwell's equation $\partial_i E_i = 0$ was used to remove possible additional terms. Notice that C_1 must be real while C_2 in general could be complex. However, the effect of the current is determined only by its divergence $\partial_i J_i$, in which only the real part of C_2 survives, as can be seen by a direct calculation. Therefore, we can take also C_2 to be real without loss of generality. At the polymer surfaces we may have an additional surface-enhanced contribution to the lateral (2D) current of zero-order in the field gradients (hence possibly stronger):

$$J_k = \left(C_s E_z^* E_k + C_s^* E_z E_k^*\right)\delta(z-L) + \left(C_i E_z^* E_k + C_i^* E_z E_k^*\right)\delta(z) \quad k = x,y \qquad \text{(S6)}$$

where C_s (C_i) is a (generally complex) constant characteristic of the polymer surface (interface with substrate) and we have introduced Dirac's delta function $\delta(z)$ to represent the surface localization of this extra current. There can be no z component of the surface current because it would imply a flow of mass out of the polymer. In addition, if Eq. (S5) predicts a nonzero z-component of the current at the polymer boundary, we must assume the presence of additional surface-specific effects (related

with the polymer cohesion energy) that will balance them. These terms will not contribute to the lateral currents, and therefore we need not find their explicit expression (they act as a constraint). Combining Eqs. (S5) and (S6), and distinguishing explicitly the *xy*-components and the *z*-one, we obtain

$$\begin{aligned} J_k &= C_1\partial_k\left(E_l^*E_l\right)+C_1\partial_k\left|E_z\right|^2+C_2\partial_l\left(E_l^*E_k+E_k^*E_l\right)+C_2\partial_z\left(E_z^*E_k+E_k^*E_z\right) \\ &+\left(C_sE_z^*E_k+C_s^*E_zE_k^*\right)\delta(z-L)+\left(C_iE_z^*E_k+C_i^*E_zE_k^*\right)\delta(z) \qquad k,l=x,y \end{aligned} \tag{S7}$$

We now average along z, across the entire polymer thickness *L*:

$$\begin{aligned} \overline{J}_k &= C_1\overline{\partial_k\left(E_l^*E_l\right)}+C_1\overline{\partial_k\left|E_z\right|^2}+C_2\overline{\partial_l\left(E_l^*E_k+E_k^*E_l\right)}+\frac{C_2}{L}\left(E_z^*E_k+E_k^*E_z\right)\Big|_0^L \\ &+\frac{1}{L}\left(C_sE_z^*E_k+C_s^*E_zE_k^*\right)_{z=L}+\frac{1}{L}\left(C_iE_z^*E_k+C_i^*E_zE_k^*\right)_{z=0} \qquad k,l=x,y \end{aligned} \tag{S8}$$

It should be noticed that the fourth term in this expression has exactly the same dependence on the fields and the thickness as the fifth and sixth ones, and may be therefore reabsorbed within them by simply redefining the constants C_s and C_i. Therefore, we drop the fourth term in the following. Moreover, we make the further assumption that the transverse fields E_x, E_y vary only little across the polymer (this corresponds to assuming that $L \ll z_0 = \pi w_0^2/\lambda$, where w_0 is the beam waist radius and λ is the wavelength) and therefore replace the averaged fields with their punctual value (at any *z* within the polymer). Within the same assumption, the two surface and interface terms will give the same effect, and we may therefore collect them by introducing a single new "boundary-related" constant

$$C_B = C_s + C_i \tag{S9}$$

After this last assumption, we obtain our final "phenomenological" expression for the averaged lateral current (corresponding to Eq. (1) of the main manuscript):

$$\overline{J}_k = C_1\partial_k\left(E_l^*E_l\right)+C_2\partial_l\left(E_l^*E_k+E_k^*E_l\right)+C_3\partial_k\left|E_z\right|^2+\frac{1}{L}\left(C_BE_z^*E_k+C_B^*E_zE_k^*\right) \qquad k,l=x,y \tag{S10}$$

In the last expression, we distinguished the third term by introducing a separate constant C_3, for increasing the generality of our treatment. From Eq. (S8) we have $C_3 = C_1$ due to 3D isotropy of the bulk polymer, but the two constants might actually become slightly different if there is some anisotropy effect along *z*. Moreover, as discussed in the main article, Eq. (S10) with three different bulk-term constants can also be derived directly from 2D symmetry considerations (i.e., isotropy in the *xy* surface), if we assume from the very beginning that the optical field does not vary significantly across *z* within the polymer. Inserting Eq. (S10) into Eq. (S4), we obtain:

$$\Delta h(x,y) = c_1\partial_k\partial_k\left(E_l^*E_l\right)+c_2\partial_k\partial_l\left(E_l^*E_k\right)+c_3\partial_k\partial_k\left|E_z\right|^2+\partial_k\left(c_BE_z^*E_k+c_B^*E_zE_k^*\right) \tag{S11}$$

in which we have introduced the constants

$$c_1 = -\frac{L\tau}{\rho}C_1$$
$$c_2 = -\frac{2L\tau}{\rho}C_2 \qquad \text{(S12)}$$
$$c_3 = -\frac{L\tau}{\rho}C_3$$
$$c_B = -\frac{\tau}{\rho}C_B$$

In a more explicit way:

$$\Delta h(x,y) = (c_1+c_2)\left[\partial_x^2\left|E_x\right|^2 + \partial_y^2\left|E_y\right|^2\right] + c_1\left(\partial_x^2\left|E_y\right|^2 + \partial_y^2\left|E_x\right|^2\right) + c_2\,\partial_x\partial_y\left(E_y^*E_x + E_x^*E_y\right)$$
$$+c_3\left(\partial_x^2\left|E_z\right|^2 + \partial_y^2\left|E_z\right|^2\right) + c_B'\left[\partial_x \mathrm{Re}\left(E_z^*E_x\right) + \partial_y \mathrm{Re}\left(E_z^*E_y\right)\right] + c_B''\left[\partial_x \mathrm{Im}\left(E_z^*E_x\right) + \partial_y \mathrm{Im}\left(E_z^*E_y\right)\right] \qquad \text{(S13)}$$

where

$$c_B' = 2\,\mathrm{Re}\left(c_B\right)$$
$$c_B'' = -2\,\mathrm{Im}\left(c_B\right)$$

The three constants C_1, C_2, C_3 are real by definition, while C_B may be complex in general. If we introduce in the model the additional assumption that all surface currents derive from electric-dipole absorption effects, proportional to $|\boldsymbol{\mu} \cdot \mathbf{E}|^2$, where $\boldsymbol{\mu}$ is a molecular transition-dipole vector, then also C_B must be real and the term with c''_B in Eq. (S13) vanishes, thus leading to Eq. (2) of the main article.

Simulated material displacement: case of Gaussian-beam illumination. Supplementary Figure S2, from S2a to S2g, reports the simulated distributions, at the focal plane of the objective, of each term of equation (2) of the main article, calculated combining the complex values of E_x, E_y and E_z obtained at the focal plane for a Gaussian light beam, linearly polarized along the *y*-axis (as for example shown in Supplementary Figure S1). The terms $\partial_x \mathrm{Re}\left(E_z^*E_x\right)$ and $\partial_y \mathrm{Re}\left(E_z^*E_y\right)$, proportional to the coefficient c_B in equation (2), are omitted because they vanish identically (actually, numerical round-off errors give to these terms random values of the order of 10^{-12} relative to the other terms). In fixing the values for the other coefficients of equation (2), the topographical surface modulation resulting from the simulation must be in agreement with that reported many times in the literature[7,8] and also reported in Fig. 2b of the main article, i.e. the two-lobed accumulation along the polarization direction. This profile is compatible with that of the function $\partial_y^2\left|E_y\right|^2$ reported in Supplementary Figure S2b. In fact, we tested several combinations for the ratios

of the coefficients c_1, c_2 and c_3, concluding that both coefficients c_1 and c_3 should be neglected to best reproduce the experimental profile. Thus, Supplementary Figures S2h and S2i report respectively the two-and three-dimensional distributions for $\Delta h(x,y)$ as derived by applying equation (2) with coefficients $c_1 = 0$, $c_2 = 1$, $c_3 = 0$. The topographical surface modulation predicted by the simulation is in complete agreement with that reported in literature. It is worth noting that the term in c_2, which represents the main component in equation (2) in this illumination conditions, is proportional to the second derivative of the intensity of a Gaussian beam linearly polarized along the *y*-axis with respect to the polarization direction. This, in fact, has motivated the past hypothesis of a mass-transport driving force proportional to the light intensity gradients[6,7,22,31]. A similar analysis can be applied to a circularly polarized Gaussian beam. The two-and three-dimensional distributions for $\Delta h(x,y)$ that we predict in this case are shown in Supplementary Figures S2l and S2j. Again, these are in excellent agreement with the experimental results reported in the literature[7,8].

Predicted material displacement: case of two-beam interference illumination. Furthermore, a configuration often considered in previous works, for large area lithographic structuring of azo-polymers, is that obtained by illumination of the sample surface with the interference pattern of two beams having equal and opposite incidence angles θ with respect to the normal of the sample surface[5,6,9,10,20]. In particular, the most frequently investigated geometries are with the beam polarizations both parallel to the incidence plane (*xz* plane), called p-p polarization combination, and both perpendicular to the incidence plane, called s-s polarization combination. In the p-p case, the intensity pattern resulting from the interference is proportional to:

$$\left|E_x\right|^2 + \left|E_z\right|^2 = 2E_0^2 + 2E_0^2 \cos(2\theta)\cos(2kx\sin\theta) \qquad \text{(S14)}$$

where E_0 is the plane-waves' amplitude and k is the wave-number. The resulting polymer relief pattern predicted by equation (2) is instead the following:

$$\begin{aligned}\Delta h &= \left(c_1 + c_2\right)\partial_x^2\left|E_x\right|^2 + c_3\partial_x^2\left|E_z\right|^2 = \\ &= -8\left(c_1 + c_2\right)E_0^2 k^2 \cos^2\theta\sin^2\theta\cos(2kx\sin\theta) + c_3 8E_0^2 k^2 \sin^4\theta\cos(2kx\sin\theta)\end{aligned} \qquad \text{(S15)}$$

If the c_2 coefficient is dominating, this pattern is π-shifted with respect to the intensity distribution (S14), as indeed observed in the experiments[5,6].

In the s-s polarization combination case the intensity distribution is given by

$$\left|E_y\right|^2 = 2E_0^2 + 2E_0^2 \cos(2kx\sin\theta) \qquad \text{(S16)}$$

and the resulting predicted relief pattern is

$$\Delta h = c_1 \partial_x^2 \left| E_y \right|^2 = -8 c_1 E_0^2 k^2 \sin^2\theta \cos(2kx\sin\theta) \qquad \text{(S17)}$$

This pattern is again π-shifted with respect to the intensity distribution, as observed in the experiments. Moreover, since it is proportional to c_1 and we have seen from other cases that this coefficient is much smaller than c_2, our model predicts that s-s relief gratings will be much smaller than p-p ones for the same exposure, as also experimentally observed.